Original Article

# FGF21 regulates insulin sensitivity following long-term chronic stress

Tomas Jelenik [1,3,6], Matthias Dille [2,3,6], Sabrina Müller-Lühlhoff [2,3,6], Dhiraj G. Kabra [2,3,6], Zhou Zhou [2,3], Christian Binsch [2,3], Sonja Hartwig [2,3], Stefan Lehr [2,3], Alexandra Chadt [2,3], Eva M.J. Peters [4], Johannes Kruse [4], Michael Roden [1,3,5], Hadi Al-Hasani [2,3,*], Tamara R. Castañeda [2,3]

## ABSTRACT

**Objective:** Post-traumatic stress disorder (PTSD) increases type 2 diabetes risk, yet the underlying mechanisms are unclear. We investigated how early-life exposure to chronic stress affects long-term insulin sensitivity.
**Methods:** C57Bl/6J mice were exposed to chronic variable stress for 15 days (Cvs) and then recovered for three months without stress (Cvs3m).
**Results:** Cvs mice showed markedly increased plasma corticosterone and hepatic insulin resistance. Cvs3m mice exhibited improved whole-body insulin sensitivity along with enhanced adipose glucose uptake and skeletal muscle mitochondrial function and fatty acid oxidation. Plasma FGF21 levels were substantially increased and associated with expression of genes involved in fatty acid oxidation and formation of brown-like adipocytes. In humans, serum FGF21 levels were associated with stress coping long time after the exposure.
**Conclusions:** Early-life exposure to chronic stress leads to long term improvements in insulin sensitivity, oxidative metabolism and adipose tissue remodeling. FGF21 contributes to a physiological memory mechanism to maintain metabolic homeostasis.
© 2018 The Authors. Published by Elsevier GmbH. This is an open access article under the CC BY-NC-ND license (http://creativecommons.org/licenses/by-nc-nd/4.0/).

**Keywords** PTSD; Chronic variable stress; Diabetes; Insulin sensitivity; FGF21; White adipose tissue

## 1. INTRODUCTION

Prolonged exposure to stress and posttraumatic stress disorders (PTSD) increase the risk for developing type 2 diabetes, cardiovascular disease and premature death [1,2]. The biological response to stress involves activation of the hypothalamic-pituitary-adrenal (HPA) and the sympathetic-adrenal-medullary (SAM) axes followed by glucocorticoid release and glucocorticoid receptor activation [3,4]. Stress can affect glucose homeostasis via glucocorticoids [5] by increasing hepatic gluconeogenesis/glycogenolysis and reducing insulin-stimulated glucose uptake in adipocyte and myocytes, either by decreased insulin signaling or glucose transporter GLUT4 abundance [6]. While hypercortisolism due to e.g. Cushing's syndrome or chronic glucocorticoid treatment associates with peripheral insulin resistance [7], the mechanisms linking stress with type 2 diabetes remain elusive. In humans, stress may cause anxiety, depression and unhealthy lifestyle, which also contribute to the development of type 2 diabetes [2]. In contrast, glucocorticoid receptor activation can decrease inflammation and improve insulin action in adipose tissue by modulating the cytokine secretory profiles [8].

Despite some knowledge about the effects of acute stress exposure or glucocorticoids on insulin action [9—11], relatively little is known about the long-term metabolic consequences following early stress exposure. Some but not all studies indicated that chronic stress may contribute to the onset and progression of type 2 diabetes [12—16]. These mixed observations could result from either different stressors, previous history of stress, or differences in post-stress environment. The latter may activate differential counter-regulatory mechanisms to revert early stress-related impairments in glucose metabolism in cohorts varying in the degree of diabetes progression. These adaptive mechanisms and associated biomarkers need to be explored, in order to develop novel therapeutic options for the prevention of stress-induced insulin resistance and type 2 diabetes.

[1]Institute for Clinical Diabetology, German Diabetes Center, Medical Faculty, Heinrich Heine University, Leibniz Center for Diabetes Research, Düsseldorf, Germany [2]Institute for Clinical Biochemistry and Pathobiochemistry, German Diabetes Center, Medical Faculty, Heinrich Heine University, Leibniz Center for Diabetes Research, Düsseldorf, Germany [3]German Center for Diabetes Research (DZD), München-Neuherberg, Germany [4]Justus-Liebig-University, Department of Psychosomatics and Psychotherapy, Psychoneuroimmunology Laboratory, Gießen, Germany [5]Division of Endocrinology and Diabetology, Medical Faculty, Heinrich Heine University, Düsseldorf, Germany

[6] These authors share equal contribution.

*Corresponding author. Institute for Clinical Biochemistry and Pathobiochemistry, German Diabetes Center (DDZ), Auf'm Hennekamp 65, 40225, Düsseldorf, Germany. E-mail: hadi.al-hasani@ddz.uni-duesseldorf.de (H. Al-Hasani).

Abbreviations: ADP, Adenosine diphosphate; AICAR, 5-Aminoimidazole-4-carboxamide ribonucleotide; BAT, brown adipose tissue; CTRL, Control; CVS, Chronic variable stress; EDL, extensor digitorum longus; EGP, endogenous glucose production; eWAT, epididymal white adipose tissue; FAO, Fatty acid oxidation; GIR, glucose infusion rate; HPA, hypothalamic-pituitary-adrenal; NEFA, non-esterified fatty acid; PTSD, Post-traumatic stress disorder; Rd, insulin-stimulated peripheral glucose disposal; ROS, reactive oxygen species; SAM, sympathetic-adrenal-medullar; WAC, white adipose cells

In the present study, we aimed at examining the effect of the chronic variable stress (Cvs) and in particular long-term metabolic adaptive mechanisms after early exposure to Cvs by using our previously established mouse model for PTSD [17] as well as in humans after an academic stress exposure. Our results identify a molecular network in which FGF21 regulates late-onset metabolic responses to stress and may account for the physiological memory mechanism to achieve metabolic homeostasis to bolster endogenous defenses against chronic variable stress.

## 2. MATERIAL AND METHODS

### 2.1. Animal study
C57BL/6J male mice (12 weeks old, Janvier, Saint Berthevin, France) were group housed under a 12:12 h light—dark cycle (06:00 h lights on) with *ad libitum* access to low-fat chow (58% carbohydrates, 33% protein, 9% fat, R/M—H Extrudat, ssniff Spezialdiäten GmbH, Soest, Germany) and tap water. All studies were carried out between 8:00 and 12:00 a.m. (light phase) based on the biological circadian rhythm of corticosterone.

### 2.2. Chronic variable stress
Age- and body weight (BW)-matched mice were subjected to a series of randomly alternating stressors (administered twice daily) over a period of 15 days [17]. The alternation of stressors prevents adaptation of the mice to particular stress intervention. Stressors were applied to each mice at the same intensity: (i) individual caging without bedding at 4 °C (1 h); (ii) swimming in 30 °C warm water (20 min); (iii) individual caging on a shaker (100 rpm, 1 h); (iv) 30 min restrain; and (v) overnight housing in a large cage. The mice subjected to Cvs were kept separately from the non-stressed controls (Ctrl) during the 15-day intervention. After Cvs intervention, all mice were transferred to the regular housing room with the Ctrl for three months (Cvs3m and Ctrl3m mice).

### 2.3. Body composition
Measurements were taken using nuclear magnetic resonance (Whole Body Composition Analyzer; Echo NRI, Houston, Texas, USA) at the end of Cvs and three months post Cvs intervention.

### 2.4. Hyperinsulinemic-euglycemic clamp
Mice underwent hyperinsulinemic-euglycemic clamps with deuterated glucose to determine whole-body and hepatic insulin sensitivity as described previously [18,19]. In brief, a silicon catheter (Silastic laboratory tubing, Dow Corning, Midland, MI) was placed into the right jugular vein under Isoflurane (CP Pharma, Burgdorf, Germany) anesthesia. Mice were allowed to recover for 4—5 days and fasted for 6 h on the day of the experiment (03:00—09:00a.m.). To assess basal whole-body glucose disposal, D-[6,6-$^2$H$_2$]glucose (98% enriched; Cambridge Isotope Laboratories, Andover, MA, USA) was infused at a rate of 4 $\mu$mol/kg/min for 120 min. The hyperinsulinemic-euglycemic clamp was performed with a primed (40 mU/kg)-continuous infusion (4 mU/kg/min; Huminsulin, Lilly, Giessen, Germany) for 180 min. Euglycemia was maintained by periodically adjusting a variable 20% glucose infusion. D-[6,6-$^2$H$_2$]glucose was co-infused together with insulin solution (0.4 $\mu$mol/kg/min) and variable glucose infusion to obtain stable tracer concentrations during varying glucose infusion rates. Blood samples were taken at 10-min intervals during the last 30 min of basal, and hyperinsulinemic-euglycemic clamps.

### 2.5. Insulin signaling
Mice were injected intraperitoneally with insulin (1 unit/kg body weight) or saline as a control and sacrificed 10 min later. Plasma and tissues were collected, snap frozen in liquid nitrogen and stored at −80 °C for further analyses.

### 2.6. Insulin-stimulated glucose uptake by white adipose cells (WAC)
Isolation of primary WAC and glucose uptake were performed as described previously [20]. Epididymal WAT was excised and pooled in 4 ml of Krebs Ringer bicarbonate HEPES (KRBH) buffer-5% (wt/vol) BSA with 2 mg/ml type I collagenase (Worthington Biochemical Corporation, Lakewood, NJ, USA). The fat pads were minced and the suspension was shaken in a water bath at 160 rpm for 50 min at 37 °C. The cells were strained through a 200 $\mu$m sterile mesh and washed twice with KRBH buffer with 5% BSA. After aspirating the wash buffer, the cells were gently re-suspended in KRBH buffer with 5% BSA to make a 10% cell suspension for glucose uptake assay. 200 $\mu$l of cell suspension was distributed into vials containing 200 $\mu$l KRBH buffer with 5% BSA with/without insulin and then incubated for 30 min at 37 °C in a gyratory bath. One hundred $\mu$l of hot medium with D-[U-$^{14}$C]glucose were added (final concentration 0.06 $\mu$Ci/ml), and the cells were incubated for another 30 min at 37 °C. After that, glucose uptake was terminated by transferring 250 $\mu$l of the cell suspension to 100 $\mu$l of dinonyl phthalate (Merck, Darmstadt, Germany) in a microcentrifuge tube. The cells were centrifuged for 10 min at 14,000 rpm. The cells (top layer) were cut away from the buffer (bottom layer) and put in scintillation tubes for radioactivity determination. Each condition was assayed in four replicates. An aliquot of the cell suspension of each group was taken before glucose uptake assay and total lipid in these cells was extracted as follow: cell suspension was firstly mixed with 2.7 ml extraction solution (80% 2-propanol, 20% N heptane, 2% sulfuric acid vol/vol), then 1.2 ml N heptane and 0.8 ml distilled water was added, after mixing by vortex, the mixture was centrifuged at 22 °C 1000 rpm for 5 min. One ml of organic phase was taken to a pre-weighed tube and dried with nitrogen. Afterwards the tube with lipid was weighed again and total lipid weight from adipocytes could be calculated. The DPM values were normalized to the corresponding lipid weight.

### 2.7. Insulin-stimulated glucose uptake and AICAR-stimulated fatty acid oxidation (FAO) in skeletal muscles
Isolation of skeletal muscles, measurements of glucose uptake and FAO were performed as described previously [20]. Extensor digitorum longus (EDL) muscles were removed from anesthetized mice and incubated for 30 min at 30 °C in vials containing pre-oxygenated (95% O2/5% CO2) Krebs-Henseleit buffer (KHB) containing 5 mM HEPES and supplemented with 5 mM glucose and 15 mM mannitol. All incubation steps were conducted under continuous gassing (95% O$_2$/5% CO$_2$) at 30 °C and slight agitation. After recovery, muscles were transferred to new vials and incubated for 30 min in KHB with 5 mM HEPES, 15 mM mannitol and 5 mM glucose under basal condition or in the presence of 120 nM insulin (Actrapid, Novo Nordisk, Mainz, Germany) throughout the duration of the experiment. Muscles were then transferred to new vials containing pre-oxygenized KHB supplemented with insulin and 15 mM mannitol and incubated for 10 min. Thereafter, muscles were transferred to new vials containing pre-oxygenized KHB supplemented with 1 mM [$^3$H]2-deoxy-glucose (2.5 mCi/ml) and 19 mM [$^{14}$C] mannitol (0.7 mCi/ml) for 20 min. Muscles were immediately frozen in liquid nitrogen and stored at −80 °C. Cleared protein lysates were used to determine incorporated radioactivity by scintillation counting. To assess palmitate oxidation, soleus muscles were incubated in pre-gassed KHB containing 15 mM mannitol, 5 mM glucose, 3.5% fatty acid-free BSA, 4 mCi/ml [$^3$H]palmitate and 600 $\mu$M unlabeled

# Original Article

palmitate with or without 2 mM AICAR (5-Aminoimidazole-4-carboxamide ribonucleotide) at 30 °C for 2 h. After absorption of fatty acids to activated charcoal, FAO was determined by scintillation measurement of tritiated water.

## 2.8. Muscle mitochondrial respiration and reactive oxygen species (ROS) emission

Ex vivo mitochondrial respiration and ROS emission was measured in freshly permeabilized soleus muscle using the Oxygraph-2k (Oroboros Instruments, Innsbruck, Austria) according to the method described previously [18,19]. Defined respiratory states were obtained by employing the following protocols: (i) tricarboxylic acid cycle (TCA)-linked respiration using 2 mM malate, 10 mM pyruvate (state 2, complex I), 2.5 mM ADP, 10 mM glutamate and (state 3, complex I), 10 mM succinate (state 3, complex I + II), 10 μM cytochrome c (mitochondrial membrane integrity check) and carbonyl cyanide-p-trifluoromethoxyphenylhydrazone (FCCP) (stepwise increments of 0.25 μM up to the final concentration of max. 1.25 μM, state u) and (ii) ß-oxidation-linked respiration using 2 mM malate, 1 mM octanoyl-carnitine (state 2, complex I + II), 2.5 mM ADP (state 3, complex I + II), 10 μM cytochrome c (mitochondrial membrane integrity check) and FCCP (stepwise increments of 0.25 μM up to the final concentration of max. 1.25 μM, state u). Addition of cytochrome c did not increase oxygen consumption indicating integrity of the outer mitochondrial membrane after saponin permeabilization.

Furthermore, the rate of ROS production was assessed simultaneously with respiration by measuring the $H_2O_2$ levels fluorometrically (O2k-Fluorescence Modul, Oroboros Instruments). In the presence of horse radish peroxidase (Sigma—Aldrich, MO, USA), Amplex Red (Amplex® Red, Invitrogen, Darmstadt, Germany) reacts with $H_2O_2$ to produce the red-fluorescent oxidation product resorufin (excitation/emission maxima of 571/585 nm, respectively). The same protocols were used as for respiration except for the addition of 5 nM oligomycin instead of cytochrome C and FCCP, to induce state 4°.

## 2.9. Tissue triglycerides

Triglyceride content was measured with Triglycerides (TRIGS) GPO-PAP Kit (Randox, Crumlin, UK) according to the manufacturer's protocol isolated from liver and muscle as described previously [20]. Frozen tissue was powdered, 20—30 mg for muscle and 10—20 mg for liver tissue and transferred into a new vial and immediately re-frozen in liquid nitrogen. In the next step 1.5 ml of a 2:1 (vol/vol) chloroform/methanol mix was added to the tissue and subsequently lysed for 4 min at 25,000 rpm via TissueLyser (Qiagen, Hilden, Germany). Triglycerides were extracted by horizontal inverting of the samples for 2 h at RT. After this time, 200 μl of ddH2O were added to the samples, mixed and centrifuged for 15 min at 3,300 × g in order to separate the upper aqueous phase from the lower organic phase. The aqueous phase was discarded and 500 μl of the organic phase transferred to a new vial. Subsequently, the chloroform was evaporated by centrifugation in a Speedvac centrifuge (Eppendorf, Hamburg, Germany) for 2 h at 22 °C. The obtained pellet was re-suspended in 1 ml of chloroform and mixed well. Subsequently, 3 × 25 μl of the suspension were transferred to new tubes to provide technical triplicates and chloroform was evaporated again. The kit's solutions were prepared prior to the assay and 150 μl per tube were added to the samples. Under occasional mixing, the samples were incubated for 10 min at 22 °C before transferring 130 μl of each tube to a 96 well plate and measurement of the triplicates was performed photometrically at a wavelength of 490 nm with a plate reader (BioRad, Munich, Germany). Subsequently, values were normalized by introduced amount of tissue.

## 2.10. Plasma analyses

Tail blood was collected in EDTA-containing tubes and centrifuged (4 °C, 3,000g, 10 min) to obtain plasma. Corticosterone was determined with the 125I radioimmunoassay (MP Biomedicals, Orangeburg, NY, USA) in plasma sampled from 4 to 5 h fasted mice between 9:00 and 10.00. FGF21 was analyzed with ELISA (R&D systems, Minneapolis, MN, USA). Plasma cholesterol (Biolatest, Erba Lachema, Karasek, Czech Republic), non-esterified fatty acid (NEFA) (Autokit NEFA C, Wako, Neuss, Germany), triglycerides (Triacylgcerols Liquid 1000, Erba Lachema, Brno, Czech Republic) and glucose (Autokit Glucose, Wako, Neuss, Germany) were assessed photometrically using enzymatic kits. Plasma hormones and cytokines were determined with multiplex immunoassays Bio-Plex Pro Mouse Diabetes 8-plex, Mouse Diabetes Adiponectin and Mouse cytokine 23-Plex using Bioplex 200 suspension array (all Biorad, Hercules, CA, USA).

## 2.11. Tissue protein expression by western blots

Tissues were lysed in RIPA-buffer (Sigma—Aldrich, MO, USA) using sonicator (Diagnode, Seraing, Belgium) and centrifuged (12,000 g, 10 min, 4 °C) [21]. Proteins in supernatants were collected and blotted for anti-phospho AKT[Ser473] (Cat# 9271), anti-AKT (Cat# 9272), anti-phospho AMPK[Thr172] (Cat# 2531), anti-AMPK (Cat# 2532), anti-Actin (Cat# 12,262), anti-GAPDH (all Cell Signaling Technologies, Cell Signaling Technology, Danvers, MA, USA), anti-UCP1 (Abcam, Cambridge, UK, ab10983) and anti-GLUT1 (Dr. A. Schürmann, Potsdam) diluted in 1x TTBS+5% BSA and incubated overnight at 4 °C under gentle agitation. Subsequently, blots were incubated with HRP-conjugated goat anti-rabbit IgG secondary antibody (Dianova, Hamburg, Germany) diluted 1:20,000 in 1x TTBS+5% BSA for 1h at room temperature. Specific protein bands were visualized using enhanced chemiluminescence reagents (Perkin Elmer, Waltham, MA, USA). Protein bands were quantified using Quantity One software (BioRad, München, Germany).

## 2.12. Real-time quantitative polymerase chain reaction (qPCR)

Total RNA was extracted from frozen tissues with the RNeasy Mini Spin Kit (Qiagen, Hilden, Germany). RNA was quantified with Nanodrop 2000 (Thermo Scientific, Wilmington, USA). cDNA templates for qPCR were synthesized from 1 μg of total RNA using the GoScript Reverse Transcription System (Promega, Madison, WI, USA). qPCR was performed using Quantifast SYBR Green PCR Kit (Promega, Madison, WI, USA). Gene expression was evaluated using the $\Delta\Delta$-Ct method and *Hprt*, *Rpl32* or *Gapdh* were used as housekeeping genes. Primer sequences are listed in Supplementary Table 4.

## 2.13. Human study

In humans, recovery from chronic stress weeks after an intense academic stress period (semester with exams that require long-term preparation) has previously been reported [22]. Briefly, female medical students were repeatedly sampled three times 10—12 weeks apart (first sample - during semester break prior to start of semester and learning for exams, second - during end of semester exams, third - after successful exam participation). Samples were taken in the morning between 8:00 and 9:00 a.m. Participants were all Caucasian, aged between 21 and 32 years, healthy, normal weighed and medication free as detailed previously [22]. Here we determined cortisol (Human Serum Kit, IBL International) and FGF21 (Human FGF-21 Quantikine ELISA Kit, R&D systems, Minneapolis, MN, USA) in analog human serum samples. Furthermore, study participants self-reported the level of perceived stress and the ability to focus on positive thoughts as a stress-coping strategy. For correlation of FGF21

with cortisol, 19 samples were available, for correlation of FGF21 with self-reported outcomes 38 samples were available.

## 2.14. Statistics

Quantitative data are presented as mean ± standard error of the mean (s.e.m.). Groups were compared with two-tailed unpaired t-tests, One-Way or Two-Way ANOVA followed by Bonferroni post hoc analysis, as stated in each figure legend. For human data, linear regressions were calculated without control for confounding factors as these were controlled for by the study design (only female sex, narrow age window, normal BMI, no lifestyle associated stress factors as reported elsewhere [22,23]). $P < 0.05$ was considered to indicate significant differences analyzed using GraphPad Prism software (La Jolla, CA, USA).

## 2.15. Study approval

The animal experiments were approved by the Ethics Committee of the State Agency for Nature, Environment and Consumer Protection (Az. 84−02.04.2011.A381; LANUV, North Rhine- Westphalia, Germany) and conducted at the animal facility of the German Diabetes Center. The human study was conducted in accordance with the Declaration of Helsinki and approved by the ethics committee of the Charité-Universitätsmedizin, Berlin, Germany, and the ethics committee of the Justus-Liebig University, Gießen, Germany. All participants in the human study provided a written informed consent approved by the institutional review board prior to inclusion in the study.

## 3. RESULTS

### 3.1. Plasma corticosterone levels increase while body weight and lean mass decrease post Cvs exposure, but not three months post-Cvs intervention

We exposed 12 weeks old male C57BL/6 mice to a random series of stressors for 15 days (Cvs) whereas corresponding unstressed mice served as controls (Ctrl) (Figure 1A). Cvs substantially increased plasma corticosterone levels (Figure 1B), decreased body weight and lean mass (Figure 1C,D) but unchanged fat mass (Figure 1E), mRNA expression of hypothalamic neuropeptide *Npy*, *Pomc* and *Agrp* (Supplementary Figure 1C) and plasma adrenaline (Supplementary Figure 1D). Adrenal weight was increased after Cvs (Supplementary Figure 1E). From 23 analyzed plasma cytokines, anti-inflammatory IL10 was increased while pro-inflammatory cytokines eotaxin and RANTES were decreased in Cvs (Supplementary Table 2). In contrast, three months post Cvs, plasma corticosterone, body weight, body composition (Figure 1F—I), expression of hypothalamic neuropeptides and plasma adrenaline (Supplementary Figure 1C) were not different between stressed mice (Cvs3m) and age-matched non-stressed controls (Ctrl3m). Colony-stimulating factor 3 in plasma was elevated, all other cytokines were not different between Cvs3m and Ctrl3m (Supplementary Table 2).

### 3.2. Cvs leads to long-term improvements in whole-body glucose disposal

Fasted plasma glucose was decreased while insulin was unchanged upon Cvs (Supplementary Figure 2). Steady-state blood glucose levels (∼120 mg/dl) during hyperinsulinemic-euglycemic clamps were similar among all groups (Figure 2A,D). Basal endogenous glucose production (EGP) was lower after Cvs (Figure 2B) in line with lower fasting blood glucose levels (Supplementary Figure 2A). Whole-body insulin-stimulated glucose disposal, expressed as glucose infusion rate (GIR), was comparable between both groups. However, insulin-mediated suppression of EGP was lower, indicating hepatic insulin

resistance, while insulin-stimulated peripheral glucose disposal (Rd) was higher in Cvs compared to Ctrl mice (Figure 2C).

Three months post Cvs, fasted plasma insulin and glucose levels were comparable between Cvs3m and Ctrl3m (Supplementary Figure 2). Basal EGP tended to be lower in Cvs3m mice ($p = 0.055$, Figure 2E). Surprisingly, GIR was higher in the Cvs3m mice (Figure 2E). This was accounted for the persistent increase in insulin-stimulated Rd (Figure 2F), while the suppression of EGP was unchanged in Cvs3m (Figure 2F). These results indicate enhanced insulin sensitivity in peripheral insulin responsive tissues, such as skeletal muscle and adipose tissue, even three months post Cvs intervention. Also intraperitoneal insulin injection led to a more pronounced decrease in plasma glucose in Cvs3m mice (Figure 2G), while the decrease in plasma NEFA was similar between Cvs3m and Ctrl3m (Figure 2H). Plasma triglycerides were not affected by insulin and were similar between Cvs3m and Ctrl3m mice (Figure 2I).

### 3.3. Cvs enhances basal fatty acid oxidation, but has no effect on the insulin-stimulated glucose uptake in skeletal muscle

We next determined glucose and lipid metabolism in *extensor digitorum longus* (EDL) skeletal muscle. Both basal and insulin-stimulated glucose uptake were similar between the Cvs and Ctrl mice (Figure 3A). Three months post Cvs exposure, both basal and insulin-stimulated glucose uptake were reduced in EDL muscle to a similar extent, but no differences were observed between muscles from Cvs3m mice and Ctrl3m animals (Figure 3B). Analysis of insulin signaling proteins revealed induction of pAKT$^{Ser473}$ in response to insulin but no differences between Cvs3m and Ctrl3m (Figure 3C,D). However, no differential activation of pAMPK$^{Thr172}$ upon insulin stimulation was observed between the different conditions (Figure 3C,E). We further explored lipid catabolism in skeletal muscle by measuring [$^3$H]palmitate oxidation in the *soleus* muscle. We observed only subtle changes in AICAR-stimulated fatty acid oxidation in the *soleus* from CVS (Figure 3F) as well as Cvs3m mice (Figure 3I). On the other hand, state 3 (ADP) ß-oxidation-linked respiration in *soleus* from Cvs mice was increased (Figure 3G), while no changes in TCA cycle-linked respiration were observed (Figure 3H). Moreover, triglycerides were unchanged in *gastrocnemius* muscle (Supplementary Figure 1A). Furthermore, both ß-oxidation-linked respiration as well as TCA-cycle-linked respiration were increased in *soleus* from Cvs3m mice (Figure 3J,K). In line with these observations, triglycerides in *gastrocnemius* muscle were decreased in Cvs3m mice (Supplementary Figure 1B). Mitochondrial mass, assessed as citrate synthase activity as well as TCA-cycle- and ß-oxidation-linked $H_2O_2$ production from permeabilized *soleus* muscle were not different among the groups (Supplementary Figure 3).

### 3.4. Enhanced insulin-stimulated glucose uptake and browning markers in white adipose cells/tissue from mice three months post Cvs intervention

In WAC, basal and insulin-stimulated glucose uptake was not different after Cvs (Figure 4A). Conversely, three months post Cvs insulin-stimulated glucose uptake was increased in WAC from Cvs3m compared to Ctrl3m (Figure 4B). Higher glucose uptake in WAC from Cvs3m mice was accompanied by the enhanced insulin signaling. Insulin-stimulated pAKT$^{Ser473}$ was markedly elevated in adipose tissue from Cvs3m mice (Figure 4C,D) in parallel with the higher GLUT1 protein (Figure 4F) and mRNA (Figure 4G) levels, while pAMPK$^{Thr172}$ (Figure 4E) and *Slc1a4* mRNA expression (Figure 4H) was unchanged. Moreover, in epididymal white adipose tissue (eWAT) from Cvs3m mice, the genes regulating adaptive thermogenesis were substantially induced, including uncoupling protein 1 (*Ucp1*), PR domain containing
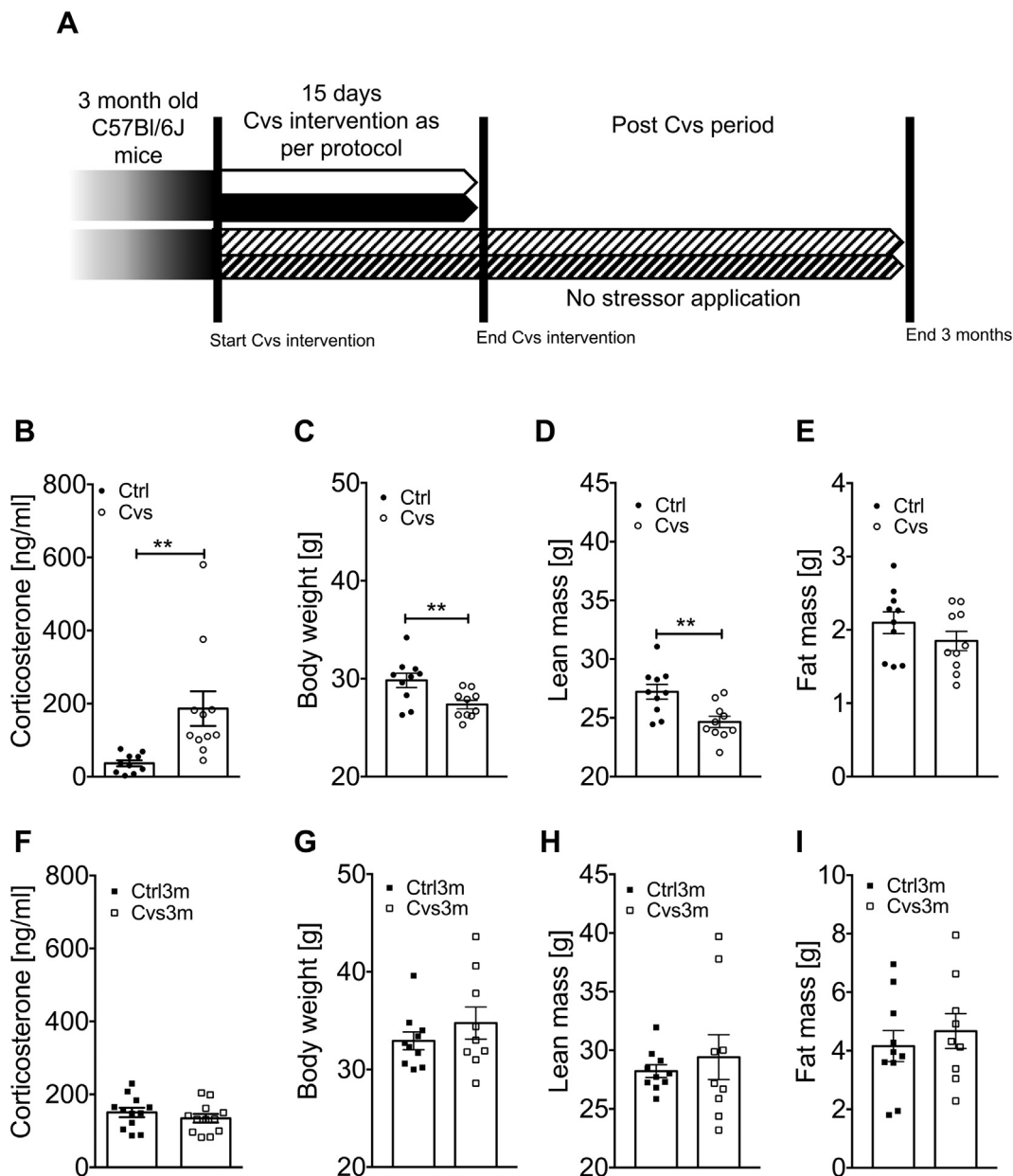
**Figure 1: Plasma corticosterone and body composition analysis from Cvs and three months post Cvs mice.** Experimental protocol: C57BL/6 male mice were exposed to chronic variable stress (Cvs) for 15 days or to no intervention (Ctrl) **(A)**. Mice underwent respective *in vivo* and *ex vivo* analyses right after Cvs intervention or three months post Cvs intervention (Cvs3m) and compared to the age-matched controls (Ctrl and Ctrl3m, respectively). Corticosterone (Cort) levels in plasma from mice fasted for 4 h **(B)** n = 10−12. Body weight, lean and fat mass data from Cvs **(C−E)** and Cvs3m mice **(F−H)** n = 9−12. Data presented as means ± s.e.m. Statistical analyses were done by two-tailed unpaired Student's t-test **(B−G)**. **p < 0.01.

16 (*Prdm16*), bone morphogenetic protein 7 (*Bmp7*), PPARG coactivator 1 alpha (*Pgc1a*), a key regulator of mitochondrial gene expression and carnitine palmitoyltransferase 1b (*Cpt1b*), a rate-limiting enzyme for fatty acid oxidation (Figure 4I).
Protein and mRNA levels of *Ucp1* were markedly increased also in brown adipose tissue (BAT) from Cvs3m mice (Figure 4J,K). Moreover, *Cpt1b* and cell death-inducing DFFA-like effector a (*Cidea*) mRNA expression were significantly increased in BAT (Figure 4K) of Cvs3m, whereas other markers of BAT activity, such as *Pgc1a*, *Bmp7*, *Cpt1a*, *Prdm16* and iodothyronine deiodinase 2 (*Dio2*) only tended to be increased (Figure 4K). Corticosterone can regulate

expression of inflammatory markers, but we found only marginal changes in the cytokines of eWAT from Cvs and Cvs3m mice (Supplementary Table 3).

### 3.5. Early exposure to Cvs leads to late onset increase in hepatic lipid content and elevation of plasma FGF21

Hepatic triglycerides were unchanged post Cvs but markedly increased three months post Cvs in Cvs3m mice (Figure 5A). Genes involved in lipogenesis including fatty acid synthase (*Fasn*), acetyl-CoA carboxylase (*Acc1, Acc2*), stearoyl-Coenzyme A desaturase (*Scd1, Scd2*) did not change in Cvs3m mice (Figure 5B). However, hepatic fatty acid
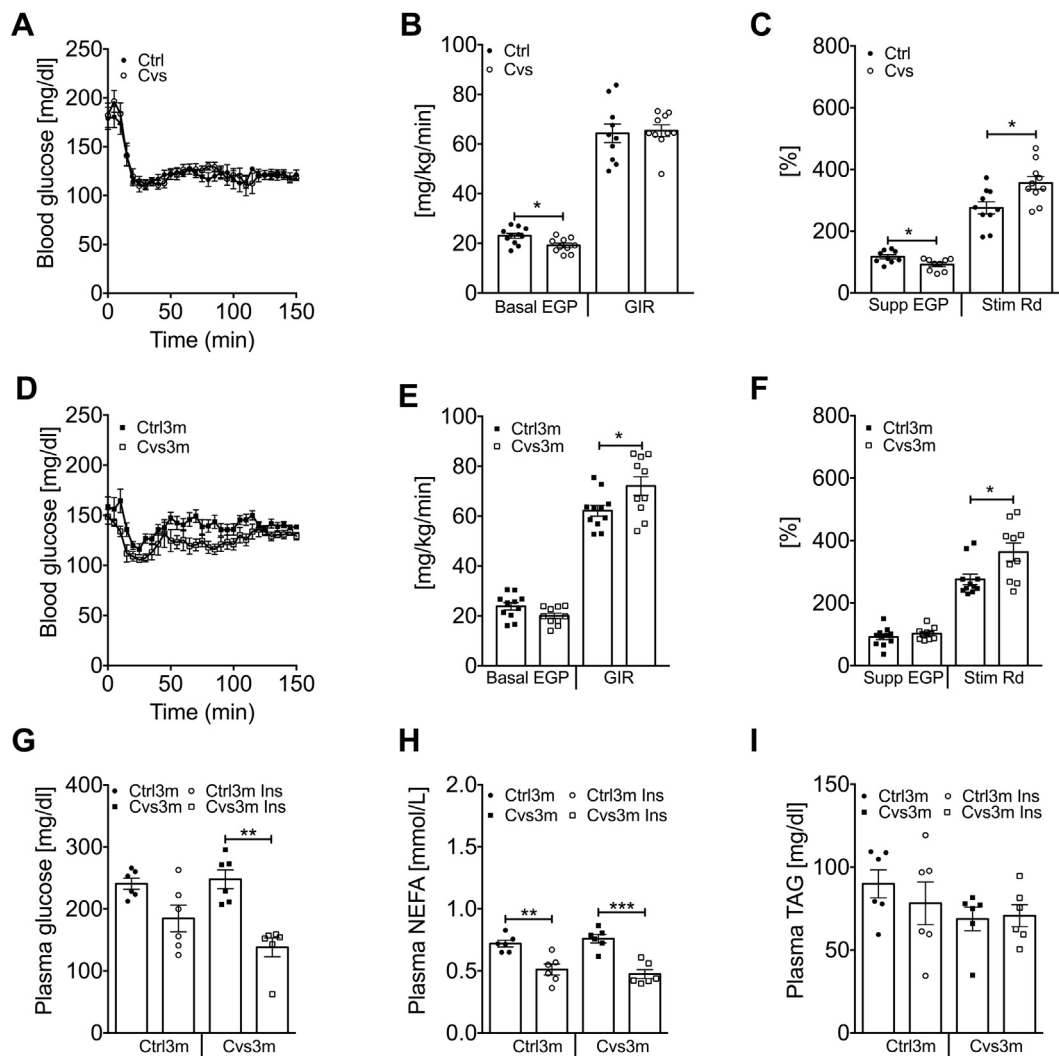
www.molecularmetabolism.com

**Figure 2:** *In vivo* insulin sensitivity analysis from Cvs and three months post Cvs mice. Blood glucose levels before and during the hyperinsulinemic-euglycemic clamp **(A, D)** n = 10−11, endogenous glucose production (EGP) and glucose infusion rate (GIR) under basal conditions **(B, E)** n = 9−11, as well as insulin-mediated suppression of EGP and stimulation of glucose disposal (Rd) **(C, F)** in mice post Cvs **(A−C)** and three months post Cvs (Cvs3m) **(D−F)** compared to the age-matched controls (Ctrl and Ctrl3m, respectively) n = 9−11. Blood biochemical parameter after bolus injection of insulin to Cvs3m and Cvs3m mice; plasma blood glucose **(G)**, plasma NEFA **(H)** and plasma triglyceride **(I)** n = 6. Data presented as means ± s.e.m. Statistical analyses were done by two-tailed unpaired Student's t-test **(A−F)** or by Two-Way ANOVA followed by Bonferroni post hoc **(G−I)**. *p < 0.05, **p < 0.01, ***p < 0.001.

translocase FAT/*Cd36* was highly upregulated in Cvs3m mice, while solute carrier family 27 (fatty acid transporter) member 5 (*Fatp5*) and fatty acid binding protein 4 (*Fabp4*) were unchanged (Figure 5C). Interestingly, we also observed increased expression of patatin like phospholipase domain containing 2 (*Pnpla2*), which catalyzes the initial step of triglyceride hydrolysis in lipid droplets (Figure 5D). Moreover, there was increased expression of *Cpt1a*, a rate limiting enzyme in fatty acid oxidation (Figure 5E).

Considering the pleiotropic effects of corticosterone on number of endocrine organs, we analyzed circulating hormones that regulate glucose homeostasis (Supplementary Table 1). Plasma FGF21 was not different right after stress exposure but showed marked elevation three months post Cvs compared to the respective control mice (Figure 5F). Furthermore, plasma FGF21 showed a positive correlation with liver triglyceride content in both Cvs3m and Ctrl3m mice (Figure 5G). In addition, we found reduced level of ghrelin and glucagon in Cvs mice,

while circulating adiponectin was lower in Cvs3m mice compared to controls (Supplementary Table 1).

### 3.6. Enhanced late onset FGF21 signaling in multiple tissues following Cvs exposure

Our data indicate that early stress exposure leads to alterations in glucose and lipid metabolism in multiple tissues, where many of these changes were previously linked to FGF21 signaling. We therefore analyzed expression of key components of FGF21 signaling in liver, skeletal muscle, BAT and WAT. FGF21 receptors and some of its downstream targets were upregulated in the liver, eWAT and BAT from Cvs3m mice, including fibroblast growth factor receptors (Fgfr) isoforms 4, 1 and 1c, *Pnpla2*, hydroxyacyl-CoA dehydrogenase (*Hadh*) and citrate synthase (*Cs*) (Figure 6A−D). Furthermore, we found elevated *Fgf21* gene expression in the liver, BAT and skeletal muscle (Figure 6E−G), indicating that these tissues are main sources of FGF21
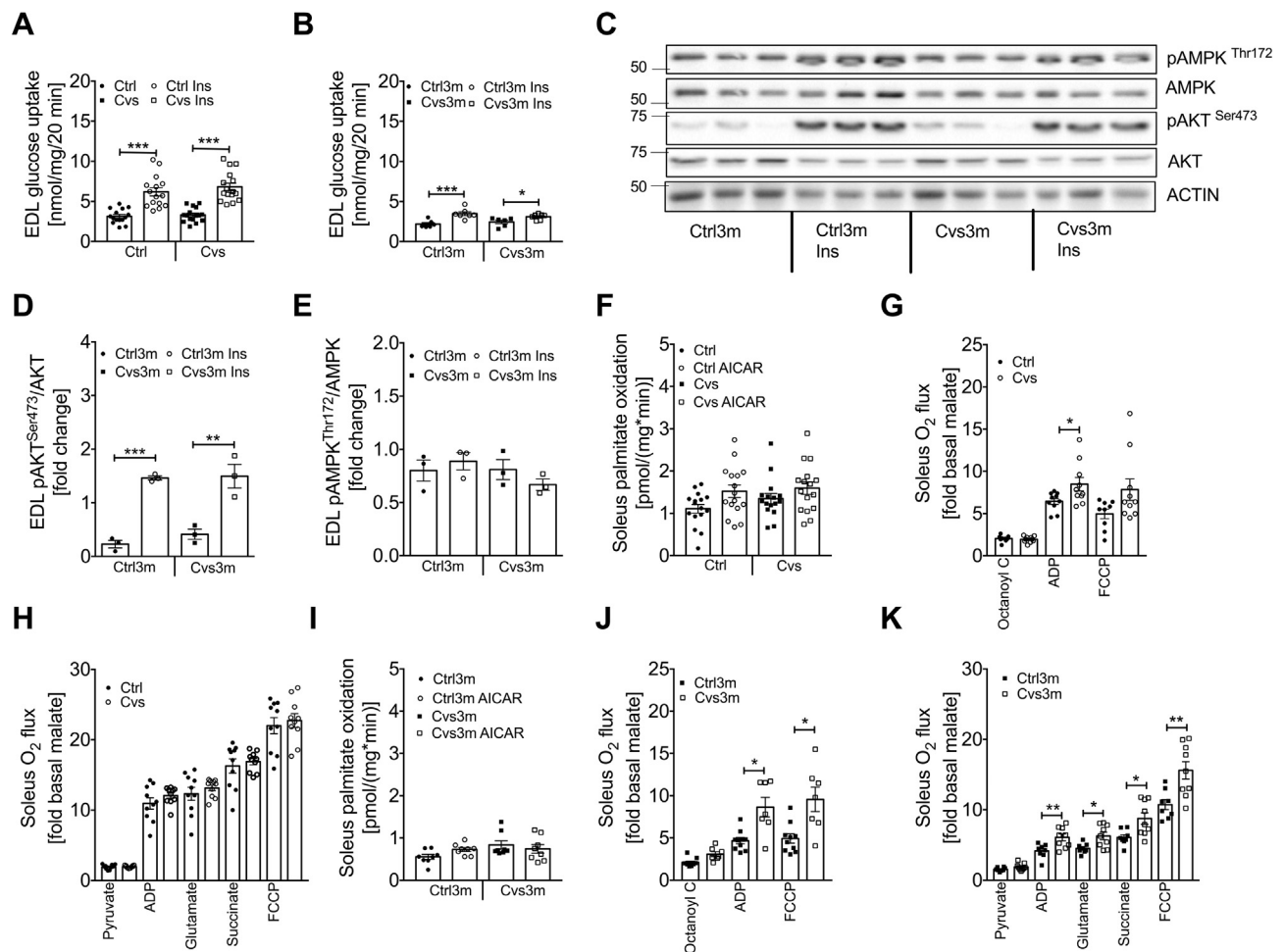
**Figure 3: Effect of Cvs and long-term effects of Cvs intervention on muscle metabolism.** *Ex vivo* glucose uptake under basal and insulin-stimulated conditions in intact isolated EDL muscle from Cvs **(A)** and three months post Cvs (Cvs3m) mice **(B)** compared to the age-matched controls (Ctrl and Ctrl3m, respectively). Representative western blot of insulin stimulated pAKT and pAMPK from EDL muscle obtained from 3 Cvs3m and Ctrl3m mice collected after *ex vivo* glucose uptake assay **(C)** and representative densitometric analysis **(D, E)**. *Ex vivo* FAO in intact isolated *Soleus* muscle under basal and AICAR-stimulated conditions **(F, I)**, ß-oxidation-linked respiration **(G, J)**, TCA-linked respiration **(H, K)** in *Soleus* muscle. Data presented as mean ± s.e.m; two-tailed unpaired Student's t-test or by Two-Way ANOVA followed by Bonferroni post hoc **(A-B, D-F and I)** *$p < 0.05$, **$p < 0.01$, ***$p < 0.001$, FAO and mitochondrial respiration $n = 7{-}18$, $n = 6{-}16$ in EDL muscle glucose uptake and $n = 3$ for western blot analysis.

three months post Cvs. In contrast, no changes in *Fgf2*1 mRNA of WAT were observed (Figure 6H).

### 3.7. Psychological stress is associated with increased FGF21 in humans

In humans, recovery from chronic stress weeks after an intense academic stress period (semester with exams that require long-term preparation) has previously been reported [22]. In order to examine the translational relevance of the data obtained in mice, we assessed FGF21 simultaneously with the cortisol in morning serum of female medical students before, at the peak of and after a defined academic stress period. Study participants were also asked to self-report the level of stress perceived and if they were able to focus their minds on positive thoughts as a stress-coping strategy. With this approach, we found that FGF21 correlated neither with cortisol nor with stress (Figure 7A—F), corresponding to the lack of an FGF21 rise in Cvs, which showed a clear rise in cortisol as an evidence of the stress response. In contrast to this lack of interaction between stress and FGF21, a striking positive correlation between FGF21 and coping was found weeks after academic stress, which was weaker prior to the

academic stress period and lacked during peak stress exposure (Figure 7G—I).

### 4. DISCUSSION

This study found that a history of stress exposure leads to a long-term metabolic adaptations with improved insulin sensitivity, specifically in adipose tissue, which could be mediated by the tissue-specific metabolic actions of FGF21.

Consistent with our previous observations, two-week exposure to Cvs intervention resulted in elevated corticosterone levels, loss of lean mass and decreased adrenal gland mass, indicating stress-induced activation of the HPA axis [17]. Moreover, hepatic insulin sensitivity was decreased and peripheral insulin sensitivity increased as measured *in vivo* with hyperinsulinemic-euglycemic clamps. These complex stress-induced alterations in insulin sensitivity are consistent with the pleiotropic effects of corticosterone on glucoregulatory insulin responsive tissues [24—27]. Previous pharmacological study in rats revealed that paraventricular nucleus mediates the dexamethasone-induced increase in Rd [27].
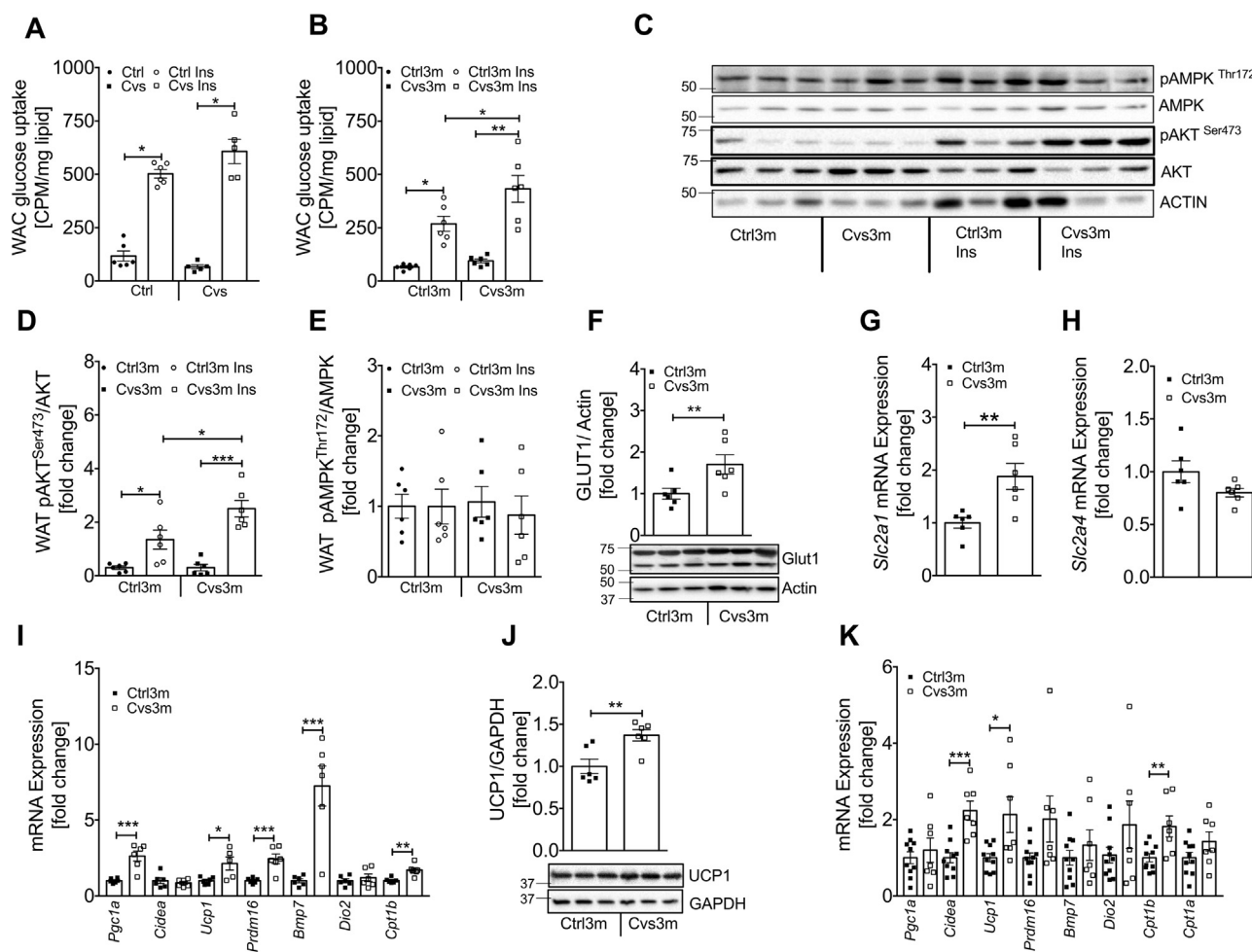
**Figure 4: Effect of Cvs and long-term effects of Cvs intervention on fat metabolism.** *Ex vivo* glucose uptake under basal and insulin-stimulated conditions in primary adipose cells from Cvs **(A)** and three months post Cvs (Cvs3m) mice **(B)** compared to the age-matched controls (Ctrl and Ctrl3m, respectively) n = 5−6. Representative white adipose tissue western blot of insulin stimulated pAKT and pAMPK **(C)** obtained from Cvs3m and Ctrl3m mice injected with insulin for 10 min and representative densitometric analysis of **(D and E)** n = 6. Representative western blot and densitometry analysis of GLUT1 **(F)** n = 6, mRNA expression analysis of *Slc2a1* (*Glut1*) **(G)**, *Slc2a4* (*Glut4*) **(H)** n = 6 and browning and thermogenic marker from eWAT following 3-month post CVS and control mice **(I)** n = 6. Representative western blot and densitometry analysis of UCP1 **(J)** n = 6 and mRNA analysis of browning and thermogenic marker from BAT from Cvs3m and Ctrl3m mice **(K)** n = 7−10. Values are means ± s.e.m. Statistical analyses were done by two-tailed unpaired Student's t-test **(F−K)** or by Two-Way ANOVA followed by Bonferroni post hoc **(A-B, D-E)**. *$p < 0.05$, **$p < 0.01$, ***$p < 0.001$.

Three months post Cvs exposure, no differences were observed in corticosterone levels, body weight, body composition and adrenal gland weight, indicating full reversibility of the acute stress effects on HPA-axis activation. Although hepatic insulin sensitivity was unchanged, peripheral insulin sensitivity remained persistently increased, altogether leading to higher whole-body insulin sensitivity in Cvs3m animals. Our *ex vivo* data indicate that skeletal muscle does not play a role in Cvs-mediated increase in Rd, as insulin-stimulated glucose uptake and AKT phosphorylation were unchanged. On the other hand, β-oxidation- and TCA cycle- linked mitochondrial respiratory capacities were elevated in the soleus muscle, which was accompanied by the lower triglyceride content. Although skeletal muscle lipid content negatively associates with insulin sensitivity and its reduction can improve glucose uptake [28], these mechanisms do not explain the increase in insulin sensitivity three months post Cvs intervention. In contrast to skeletal muscle, insulin-stimulated glucose uptake as well as AKT phosphorylation and GLUT1 expression were increased in adipocytes from Cvs3m mice, strongly indicating that elevated glucose metabolism of adipose tissue underlies the improvements in the

whole-body insulin sensitivity three months post Cvs. Moreover, WAT from Cvs3m mice showed enhanced expression of key regulators of browning and thermogenic markers. Browning of adipose tissue and increased thermogenesis have been inversely related to insulin resistance [29] and might protect from obesity and lipid-mediated impairments of glucose metabolism [30]. Similar mechanisms could indirectly contribute to the improved glucose metabolism also in Cvs3m mice. Furthermore, we found only a moderate increase of triglycerides and unchanged insulin sensitivity in the liver of Cvs3m mice. High levels of hepatic lipids were accompanied by induced mRNA levels of the fatty acid transporter *Cd36* but unchanged expression of genes involved in *de novo* lipogenesis. A previous study supports our findings by showing that chronically elevated corticosterone exacerbates hepatic steatosis via induction of *Cd36* in high-fat diet fed mice [31].

The question remains, which mechanisms mediate the above-described, tissue-specific metabolic effects of Cvs three months after the exposure. The analysis of circulating metabolic hormones and cytokines, which have been linked to the regulation of glucose
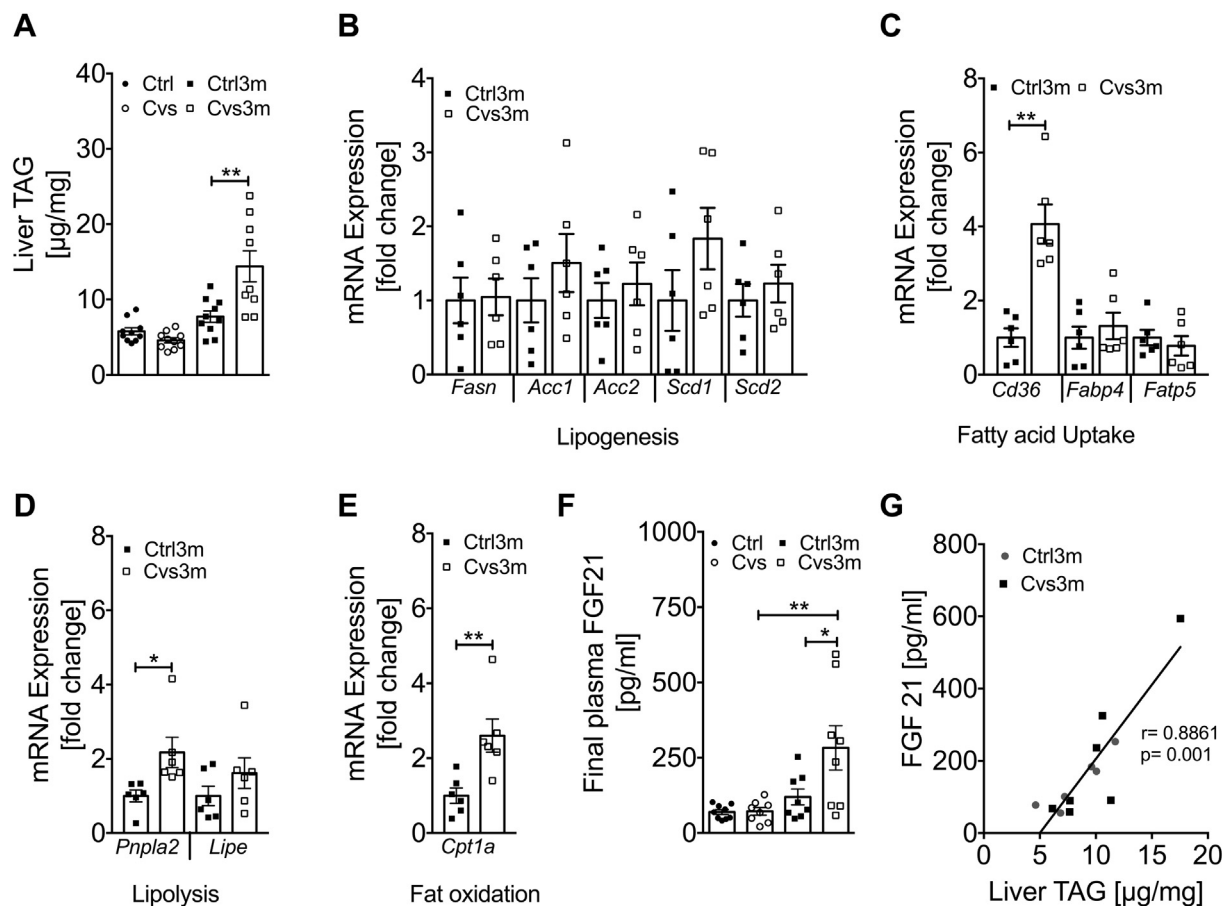
**Figure 5: Enhanced liver triglyceride (TAG) content positively correlates with FGF21 secretion in mice three months post Cvs.** Liver TAG content from Cvs and three months post Cvs (Cvs3m) mice **(A)** compared to the age-matched controls (Ctrl and Ctrl3m, respectively) n = 9–10. mRNA expression of gene associated with lipogenesis **(B)**, fatty acid uptake **(C)**, lipolysis **(D)** and fat oxidation **(E)** from Cvs3m and Ctrl3m mice n = 6. Plasma level of FGF21 **(F)** n = 8–9 and correlation analysis of plasma FGF21 and liver TAG content **(G)** n = 6–7. Values are means ± s.e.m. Statistical analyses were done by two-tailed unpaired Student's t-test **(B–E)** or by Two-Way ANOVA followed by Bonferroni post hoc **(A and F)**. *p < 0.05, **p < 0.01. r is representing Pearson correlation.

homeostasis, revealed a substantial increase in plasma FGF21. Previous studies identified the liver as primary source of FGF21 secretion [32–35] and FGF21 positively correlated with hepatic fat content in patients with non-alcoholic fatty liver disease [36]. Consistent with these data, we found increased hepatic *Fgf21* expression and a strong correlation between plasma FGF21 and hepatic triglycerides. Moreover, some studies have shown a strong association of glucocorticoid receptor activation with induction of FGF21 [37–39]. We speculate that late-onset FGF21 expression might constitute part of an adaptive mechanism for protection from glucocorticoid-induced hepatic lipid accumulation. On the other hand, exposure to stress and PTSD have been linked to the epigenetic modifications of genes involved in various physiological pathways [40]. Thus, epigenetic alterations in the *Fgf21* DNA could also mediate the late-onset effects of stress on FGF21 expression and insulin sensitivity, as supported by previous studies. For example, environmental changes, such as altered nutritional composition, induced *Fgf21* methylation in mouse liver [41]. Recent studies showed that, in addition to liver as a source for FGF21, skeletal muscle may also secrete FGF21 under conditions of metabolic stress [42–48] and adipose tissue upon cold exposure or *Ucp1* overexpression [49,50]. We extend these findings by showing markedly increased expression of *Fgf21* in skeletal muscle and brown adipose tissue three months after Cvs intervention.

FGF21 has known beneficial effects on glucose metabolism, which has been shown in various models [33,35,36,49,51]. Multiple pathways in insulin-responsive tissues that are targets of FGF21 were affected also in Cvs3m mice. For example, expression of FGF21 receptors was induced in the liver, WAT and BAT, indicating increased FGF21-associated signaling in these tissues. Indeed, hepatic expression of downstream FGF21 targets of lipolysis and fatty acid oxidation was increased. Importantly, FGF21 could mediate the increased glucose uptake via induction of GLUT1 in WAT, as supported by previously described mechanistic link between FGF21 and GLUT1 expression in adipocytes [52]. In addition to the acute effects on glucose disposal, FGF21 has been associated with WAT browning [49]. Also, Cvs3m mice showed enhanced expression of key regulators of browning, thermogenesis and fatty acid oxidation, indicating that FGF21-driven browning of WAT could contribute to the insulin-sensitizing effect in response to stress. In addition to WAT, FGF21 can regulate BAT activity and fatty acid metabolism in skeletal muscle [48,49], which have been changed accordingly in Cvs3m mice. Collectively, all these observations demonstrate that high circulating FGF21 levels associate with induction of multiple FGF21-regulated pathways, which could contribute to the improved insulin sensitivity following long-term chronic stress.

In order to address translational aspect of our observations in mice, we analyzed serum FGF21 levels in humans recovering from academic stress,
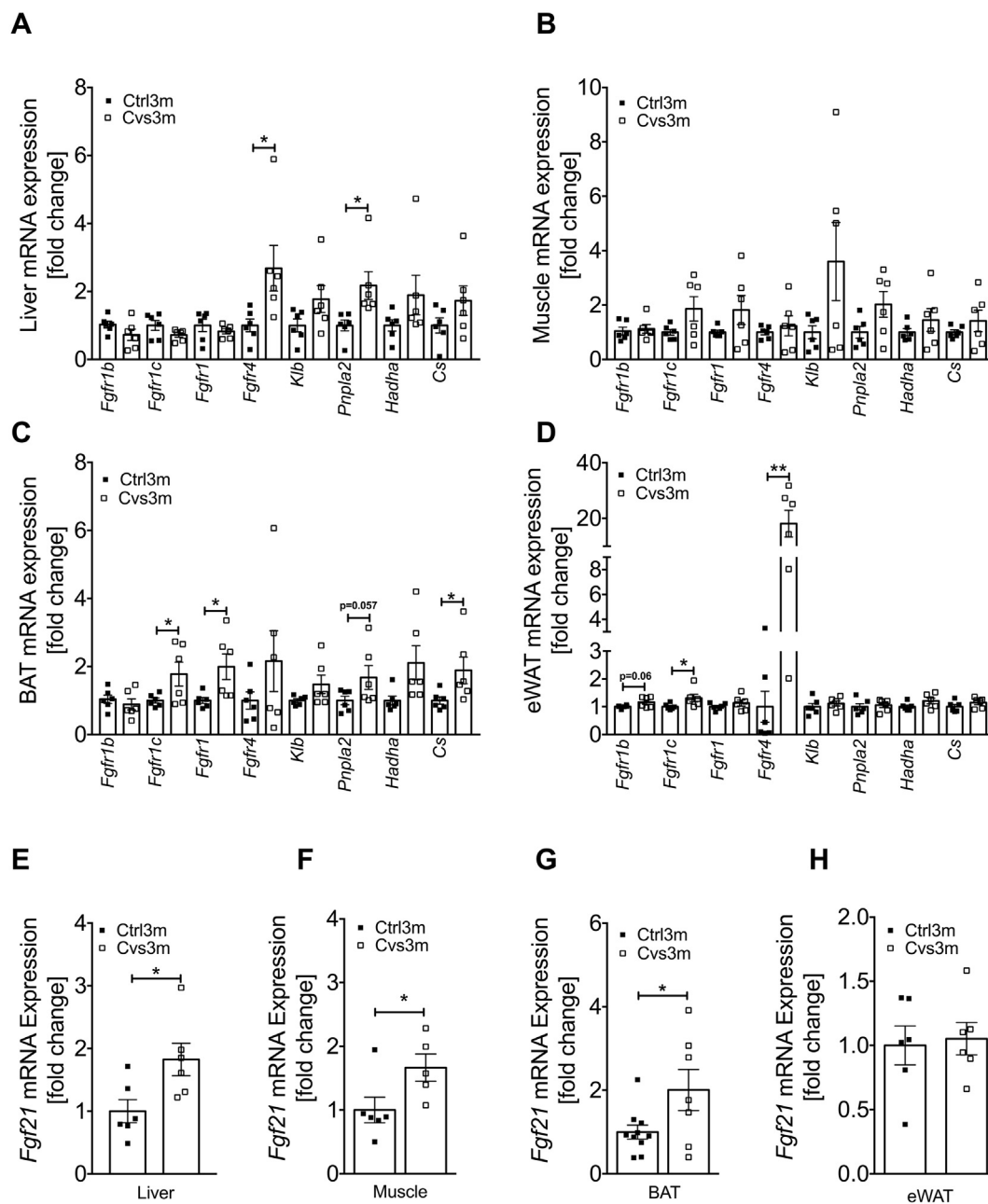
www.molecularmetabolism.com

**Figure 6: Induction of *Fgf21* mRNA expression along with FGF21 regulated gene in metabolic tissue from mice three months post Cvs.** mRNA expression analysis of FGF21 regulated key genes from liver **(A)**, *gastrocnemius* muscle **(B)**, BAT **(C)** and eWAT **(D)** from mice three months post Cvs (Cvs3m) and age-matched control (Ctrl3m) mice n = 6. mRNA expression of *Fgf21* from liver **(E)**, *gastrocnemius* muscle **(F)**, BAT **(G)** and eWAT **(H)** from Cvs3m and Ctrl3m mice n = 5−10. Values are means ± s.e.m. Statistical analyses were done by two-tailed unpaired Student's t-test between group **(A—H)**. *$p < 0.05$, **$p < 0.01$.

who are characterized by high levels of cortisol and altered insulin sensitivity. We found no association of FGF21 with cortisol or with stress, while there was a positive correlation between FGF21 and ability to cope with stress weeks after academic stress. These results support the hypothesis that stress relates to FGF21 secretion even long time after the exposure to stress and show that FGF21 could mediate the late stress-induced adaptive effects on the glucose and lipid metabolism also in humans.

## 5. CONCLUSIONS

Exposure to stress is followed by tissue-specific adaptations of lipid and glucose metabolism, and these changes can occur long after the

stress exposure. In particular, peripheral insulin sensitivity is improved due to increased insulin signaling and glucose uptake in WAT. Furthermore, adipose tissue browning and thermogenesis as well as increased fatty acid oxidation in the muscle contribute to the improved whole-body insulin sensitivity. Circulating levels of FGF21 are increased and positively correlate with the hepatic lipid content. Metabolic changes are highly consistent with increased FGF21-associated signaling in multiple insulin-sensitive tissues. The significance of our observations in mice is underlined by the association of serum FGF21 and ability to cope with stress in humans long after exposure to academic stress. Our findings highlight the relevance of FGF21 in adaptation to metabolic and physiological stress and may
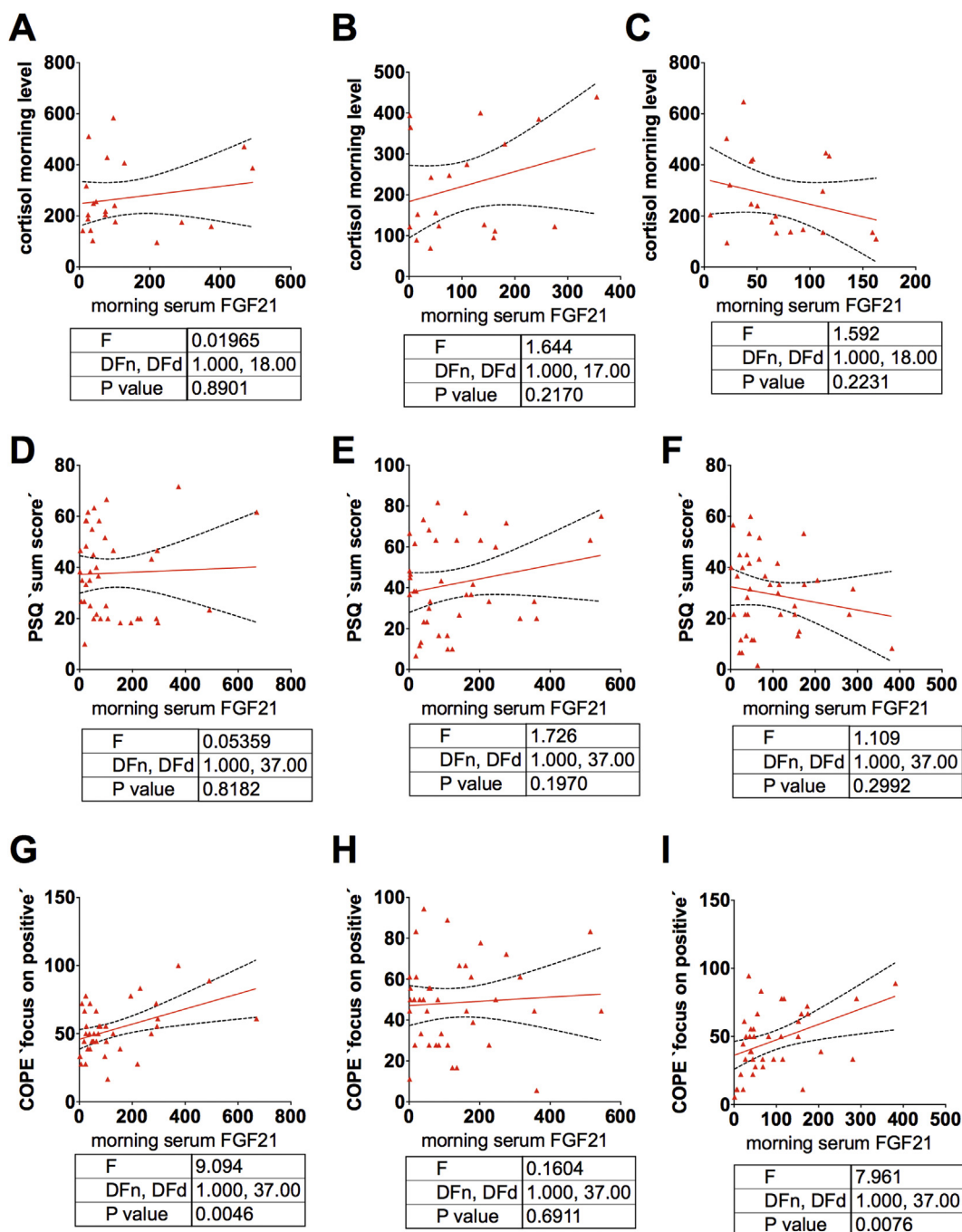
**Figure 7: Translational association of chronic variable stress with FGF21.** Interaction between FGF21 serum levels and cortisol morning serum levels **(A—C)** as well as self-reported stress **(D—F)** and coping **(G—I)** as a marker for resilience in medical students during semester break **(A, D and G)**, end of semester exam period **(B, E and H)** and 10—12 weeks after successful exams **(C, F and I)**. A, n = 19; B and C, n = 38. Results of linear regression analysis are shown.

have clinical implications for the prediction for type 2 diabetes in individuals exposed to or having previous history of stress.

## AUTHOR CONTRIBUTIONS

TJ conceived, designed and performed experiments, analyzed data and wrote the manuscript. MD, SML performed experiments, analyzed data and edited the manuscript. DGK conceived, designed and performed experiments, analyzed data and wrote the manuscript. ZZ performed and analyzed fatty acid uptake experiment. CB performed the Cvs animal experiments. SH, SL designed and performed multiplex ELISA, analyzed data and edited the manuscript. AC designed and performed glucose uptake assay, analyzed data and edited the manuscript. EMP, JK performed human experiments, analyzed data and edited the manuscript. MR and HA conceived and designed the experiments and wrote the manuscript. HA is the guarantor of this work. TRC conceived, designed and performed experiments, analyzed data and wrote the manuscript.

## CONFLICT OF INTEREST

All authors have declared that no conflict of interest exists.

## APPENDIX A. SUPPLEMENTARY DATA

Supplementary data related to this article can be found at https://doi.org/10.1016/j.molmet.2018.06.012.

## REFERENCES

[1] Boscarino, J.A., 2004. Posttraumatic stress disorder and physical illness: results from clinical and epidemiologic studies. Annals of the New York Academy of Sciences 1032:141—153.

[2] Pouwer, F., Kupper, N., Adriaanse, M.C., 2010. Does emotional stress cause type 2 diabetes mellitus? A review from the European Depression in Diabetes (EDID) Research Consortium. Discovery Medicine 9:112—118.

[3] Bamberger, C.M., Schulte, H.M., Chrousos, G.P., 1996. Molecular determinants of glucocorticoid receptor function and tissue sensitivity to glucocorticoids. Endocrine Reviews 17:245—261.

[4] Munck, A., Guyre, P.M., Holbrook, N.J., 1984. Physiological functions of glucocorticoids in stress and their relation to pharmacological actions. Endocrine Reviews 5:25—44.

[5] Sapolsky, R.M., Romero, L.M., Munck, A.U., 2000. How do glucocorticoids influence stress responses? Integrating permissive, suppressive, stimulatory, and preparative actions. Endocrine Reviews 21:55—89.

[6] Kuo, T., McQueen, A., Chen, T.C., Wang, J.C., 2015. Regulation of glucose homeostasis by glucocorticoids. Advances in Experimental Medicine & Biology 872:99—126.

[7] Nosadini, R., Del Prato, S., Tiengo, A., Valerio, A., Muggeo, M., Opocher, G., et al., 1983. Insulin resistance in Cushing's syndrome. The Journal of Cinical Endocrinology and Metabolism 57:529—536.

[8] Geer, E.B., Islam, J., Buettner, C., 2014. Mechanisms of glucocorticoid-induced insulin resistance: focus on adipose tissue function and lipid metabolism. Endocrinology and Metabolism Clinics of North America 43:75—102.

[9] Laskewitz, A.J., van Dijk, T.H., Bloks, V.W., Reijngoud, D.J., van Lierop, M.J., Dokter, W.H., et al., 2010. Chronic prednisolone treatment reduces hepatic insulin sensitivity while perturbing the fed-to-fasting transition in mice. Endocrinology 151:2171—2178.

[10] Moberg, E., Kollind, M., Lins, P.E., Adamson, U., 1994. Acute mental stress impairs insulin sensitivity in IDDM patients. Diabetologia 37:247—251.

[11] Nowotny, B., Cavka, M., Herder, C., Loffler, H., Poschen, U., Joksimovic, L., et al., 2010. Effects of acute psychological stress on glucose metabolism and subclinical inflammation in patients with post-traumatic stress disorder. Hormone and Metabolic Research 42:746—753.

[12] Faulenbach, M., Uthoff, H., Schwegler, K., Spinas, G.A., Schmid, C., Wiesli, P., 2012. Effect of psychological stress on glucose control in patients with Type 2 diabetes. Diabetic Medicine 29:128—131.

[13] Naliboff, B.D., Cohen, M.J., Sowers, J.D., 1985. Physiological and metabolic responses to brief stress in non-insulin dependent diabetic and control subjects. Journal of Psychosomatic Research 29:367—374.

[14] Packard, A.E., Ghosal, S., Herman, J.P., Woods, S.C., Ulrich-Lai, Y.M., 2014. Chronic variable stress improves glucose tolerance in rats with sucrose-induced prediabetes. Psychoneuroendocrinology 47:178—188.

[15] Pibernik-Okanovic, M., Roglic, G., Prasek, M., Metelko, Z., 1993. War-induced prolonged stress and metabolic control in type 2 diabetic patients. Psychological Medicine 23:645—651.

[16] Reynolds, R.M., Labad, J., Strachan, M.W., Braun, A., Fowkes, F.G., Lee, A.J., et al., 2010. Elevated fasting plasma cortisol is associated with ischemic heart disease and its risk factors in people with type 2 diabetes: the Edinburgh type 2 diabetes study. The Journal of Cinical Endocrinology and Metabolism 95: 1602—1608.

[17] Castaneda, T.R., Nogueiras, R., Muller, T.D., Krishna, R., Grant, E., Jones, A., et al., 2011. Decreased glucose tolerance and plasma adiponectin:resistin ratio in a mouse model of post-traumatic stress disorder. Diabetologia 54: 900—909.

[18] Jelenik, T., Kaul, K., Sequaris, G., Flogel, U., Phielix, E., Kotzka, J., et al., 2017. Mechanisms of insulin resistance in primary and secondary nonalcoholic fatty liver. Diabetes 66:2241—2253.

[19] Jelenik, T., Sequaris, G., Kaul, K., Ouwens, D.M., Phielix, E., Kotzka, J., et al., 2014. Tissue-specific differences in the development of insulin resistance in a mouse model for type 1 diabetes. Diabetes 63:3856—3867.

[20] Chadt, A., Immisch, A., de Wendt, C., Springer, C., Zhou, Z., Stermann, T., et al., 2015. Deletion of both Rab-GTPase-activating proteins TBC1D1 and TBC1D4 in mice eliminates insulin- and AICAR-stimulated glucose transport [corrected]. Diabetes 64:746—759.

[21] Kabra, D.G., Pfuhlmann, K., Garcia-Caceres, C., Schriever, S.C., Casquero Garcia, V., Kebede, A.F., et al., 2016. Hypothalamic leptin action is mediated by histone deacetylase 5. Nature Communications 7:10782.

[22] Harb, H., Gonzalez-de-la-Vara, M., Thalheimer, L., Klein, U., Renz, H., Rose, M., et al., 2017. Assessment of Brain Derived Neurotrophic Factor in hair to study stress responses: a pilot investigation. Psychoneuroendocrinology 86: 134—143.

[23] Peters, E., Shoots-Reinhard, B., Tompkins, M.K., Schley, D., Meilleur, L., Sinayev, A., et al., 2017. Improving numeracy through values affirmation enhances decision and STEM outcomes. PLoS One 12:e0180674.

[24] Hong, E.G., Ko, H.J., Cho, Y.R., Kim, H.J., Ma, Z., Yu, T.Y., et al., 2009. Interleukin-10 prevents diet-induced insulin resistance by attenuating macrophage and cytokine response in skeletal muscle. Diabetes 58: 2525—2535.

[25] Nilsson, C., Jennische, E., Ho, H.P., Eriksson, E., Bjorntorp, P., Holmang, A., 2002. Increased insulin sensitivity and decreased body weight in female rats after postnatal corticosterone exposure. European Journal of Endocrinology 146:847—854.

[26] Vander Kooi, B.T., Onuma, H., Oeser, J.K., Svitek, C.A., Allen, S.R., Vander Kooi, C.W., et al., 2005. The glucose-6-phosphatase catalytic subunit gene promoter contains both positive and negative glucocorticoid response elements. Molecular Endocrinology 19:3001—3022.

[27] Yi, C.X., Foppen, E., Abplanalp, W., Gao, Y., Alkemade, A., la Fleur, S.E., et al., 2012. Glucocorticoid signaling in the arcuate nucleus modulates hepatic insulin sensitivity. Diabetes 61:339—345.

[28] Ritter, O., Jelenik, T., Roden, M., 2015. Lipid-mediated muscle insulin resistance: different fat, different pathways? Journal of Molecular Medicine (Berlin) 93:831—843.

[29] Lo, K.A., Sun, L., 2013. Turning WAT into BAT: a review on regulators controlling the browning of white adipocytes. Bioscience Reports 33.

[30] Vitali, A., Murano, I., Zingaretti, M.C., Frontini, A., Ricquier, D., Cinti, S., 2012. The adipose organ of obesity-prone C57BL/6J mice is composed of

mixed white and brown adipocytes. The Journal of Lipid Research 53: 619—629.

[31] D'Souza, A.M., Beaudry, J.L., Szigiato, A.A., Trumble, S.J., Snook, L.A., Bonen, A., et al., 2012. Consumption of a high-fat diet rapidly exacerbates the development of fatty liver disease that occurs with chronically elevated glucocorticoids. American Journal of Physiology — Gastrointestinal and Liver Physiology 302:G850—G863.

[32] Badman, M.K., Koester, A., Flier, J.S., Kharitonenkov, A., Maratos-Flier, E., 2009. Fibroblast growth factor 21-deficient mice demonstrate impaired adaptation to ketosis. Endocrinology 150:4931—4940.

[33] Emanuelli, B., Vienberg, S.G., Smyth, G., Cheng, C., Stanford, K.I., Arumugam, M., et al., 2014. Interplay between FGF21 and insulin action in the liver regulates metabolism. Journal of Clinical Investigation 124:515—527.

[34] Inagaki, T., Dutchak, P., Zhao, G., Ding, X., Gautron, L., Parameswara, V., et al., 2007. Endocrine regulation of the fasting response by PPARalpha-mediated induction of fibroblast growth factor 21. Cell Metabolism 5:415—425.

[35] Ohta, H., Konishi, M., Itoh, N., 2011. FGF10 and FGF21 as regulators in adipocyte development and metabolism. Endocrine, Metabolic & Immune Disorders — Drug Targets 11:302—309.

[36] Li, H., Fang, Q., Gao, F., Fan, J., Zhou, J., Wang, X., et al., 2010. Fibroblast growth factor 21 levels are increased in nonalcoholic fatty liver disease patients and are correlated with hepatic triglyceride. Journal of Hepatology 53:934—940.

[37] Marino, J.S., Stechschulte, L.A., Stec, D.E., Nestor-Kalinoski, A., Coleman, S., Hinds Jr., T.D., 2016. Glucocorticoid receptor beta induces hepatic steatosis by augmenting inflammation and inhibition of the peroxisome proliferator-activated receptor (PPAR) alpha. Journal of Biological Chemistry 291: 25776—25788.

[38] Patel, R., Bookout, A.L., Magomedova, L., Owen, B.M., Consiglio, G.P., Shimizu, M., et al., 2015. Glucocorticoids regulate the metabolic hormone FGF21 in a feed-forward loop. Molecular Endocrinology 29:213—223.

[39] Vispute, S.G., Bu, P., Le, Y., Cheng, X., 2017. Activation of GR but not PXR by dexamethasone attenuated acetaminophen hepatotoxicities via Fgf21 induction. Toxicology 378:95—106.

[40] Roth, T.L., 2014. How traumatic experiences leave their signature on the genome: an overview of epigenetic pathways in PTSD. Frontiers in Psychiatry 5:93.

[41] Yuan, X., Tsujimoto, K., Hashimoto, K., Kawahori, K., Hanzawa, N., Hamaguchi, M., et al., 2018. Epigenetic modulation of Fgf21 in the perinatal mouse liver ameliorates diet-induced obesity in adulthood. Nature Communications 9:636.

[42] Crooks, D.R., Natarajan, T.G., Jeong, S.Y., Chen, C., Park, S.Y., Huang, H., et al., 2014. Elevated FGF21 secretion, PGC-1alpha and ketogenic enzyme expression are hallmarks of iron-sulfur cluster depletion in human skeletal muscle. Human Molecular Genetics 23:24—39.

[43] Guridi, M., Tintignac, L.A., Lin, S., Kupr, B., Castets, P., Ruegg, M.A., 2015. Activation of mTORC1 in skeletal muscle regulates whole-body metabolism through FGF21. Science Signaling 8:ra113.

[44] Harris, L.A., Skinner, J.R., Shew, T.M., Pietka, T.A., Abumrad, N.A., Wolins, N.E., 2015. Perilipin 5-driven lipid droplet accumulation in skeletal muscle stimulates the expression of fibroblast growth factor 21. Diabetes 64: 2757—2768.

[45] Izumiya, Y., Bina, H.A., Ouchi, N., Akasaki, Y., Kharitonenkov, A., Walsh, K., 2008. FGF21 is an Akt-regulated myokine. FEBS Letters 582:3805—3810.

[46] Kim, K.H., Jeong, Y.T., Oh, H., Kim, S.H., Cho, J.M., Kim, Y.N., et al., 2013. Autophagy deficiency leads to protection from obesity and insulin resistance by inducing Fgf21 as a mitokine. Nature Medicine 19:83—92.

[47] Ost, M., Coleman, V., Voigt, A., van Schothorst, E.M., Keipert, S., van der Stelt, I., et al., 2016. Muscle mitochondrial stress adaptation operates independently of endogenous FGF21 action. Molecular Metabolism 5:79—90.

[48] Vandanmagsar, B., Warfel, J.D., Wicks, S.E., Ghosh, S., Salbaum, J.M., Burk, D., et al., 2016. Impaired mitochondrial fat oxidation induces FGF21 in muscle. Cell Reports 15:1686—1699.

[49] Fisher, F.M., Kleiner, S., Douris, N., Fox, E.C., Mepani, R.J., Verdeguer, F., et al., 2012. FGF21 regulates PGC-1alpha and browning of white adipose tissues in adaptive thermogenesis. Genes & Development 26:271—281.

[50] Keipert, S., Kutschke, M., Lamp, D., Brachthauser, L., Neff, F., Meyer, C.W., et al., 2015. Genetic disruption of uncoupling protein 1 in mice renders brown adipose tissue a significant source of FGF21 secretion. Molecular Metabolism 4:537—542.

[51] Potthoff, M.J., Inagaki, T., Satapati, S., Ding, X., He, T., Goetz, R., et al., 2009. FGF21 induces PGC-1alpha and regulates carbohydrate and fatty acid metabolism during the adaptive starvation response. Proceedings of the National Academy of Sciences of the U S A 106:10853—10858.

[52] Ge, X., Chen, C., Hui, X., Wang, Y., Lam, K.S., Xu, A., 2011. Fibroblast growth factor 21 induces glucose transporter-1 expression through activation of the serum response factor/Ets-like protein-1 in adipocytes. Journal of Biological Chemistry 286:34533—34541.